

Assessment of the imprinting efficiency of an imide with a
“stoichiometric” pyridinebased functional monomer in

Original

Assessment of the imprinting efficiency of an imide with a
“stoichiometric” pyridinebased functional monomer in
precipitation polymerisation / Fremiella Lim, K.; Hall, Andrew J.; Lettieri, Stefania; Holdsworth, Clovia I.. - In: JOURNAL
OF MOLECULAR RECOGNITION. - ISSN 0952-3499. - ELETTRONICO. - 31:3(2017). [10.1002/jmr.2655]

Availability:

This version is available at: 11583/2979312 since: 2023-06-12T07:43:22Z

Publisher:

WILEY

Published

DOI:10.1002/jmr.2655

Terms of use:

This article is made available under terms and conditions as specified in the corresponding bibliographic description in
the repository

Publisher copyright

(Article begins on next page)

SPECIAL ISSUE ARTICLE

Assessment of the imprinting efficiency of an imide with a “stoichiometric” pyridine-based functional monomer in precipitation polymerisation

K. Fremielle Lim¹ | Andrew J. Hall² | Stefania Lettieri^{2,3} | Clovia I. Holdsworth¹ 

¹Discipline of Chemistry, School of Environmental and Life Sciences, University of Newcastle, Callaghan, New South Wales 2308, Australia

²Medway School of Pharmacy, Universities of Greenwich and Kent at Medway, Anson Building, Central Avenue, Chatham Maritime, Chatham, Kent ME4 4TB, UK

³Istituto Italiano di Tecnologia, Via Morego, 30, 16163 Genoa, Italy

Correspondence

Clovia I. Holdsworth, Discipline of Chemistry, School of Environmental and Life Sciences, University of Newcastle, Callaghan, New South Wales 2308 Australia.

Email: clovia.holdsworth@newcastle.edu.au

Abstract

The efficiency of the stoichiometric non-covalent imprinting of the imide 2,3,5-tri-*O*-acetyluridine (TAU) with 2,6-bis(acrylamido)pyridine (BAAPy) as functional monomer due to their strong donor-acceptor-donor/acceptor-donor-acceptor (DAD/ADA) hydrogen bond array interaction has been evaluated by bulk imprinting. This study is the first to investigate the imprinting and template rebinding efficiencies of the TAU/BAAPy molecularly imprinted polymeric (MIP) system prepared by precipitation polymerisation. We found that the stoichiometric 1:1 T:FM ratio has not been maintained in precipitation polymerisation and an optimal TAU:BAAPy ratio of 1:2.5 was obtained in acetonitrile without agitation affording an affinity constant ($1.7 \times 10^4 \text{ M}^{-1}$) and a binding capacity (3.69 $\mu\text{mol/g}$) higher than its bulk counterpart. Molecular modelling, NMR studies, and selectivity assays against analogues uridine and 2,3,5-tri-*O*-acetyl cytidine (TAC) indicate that, aside from the DAD/ADA hydrogen bond interaction, BAAPy also interacts with the acetyl groups of TAU. Template incorporation and rebinding in precipitation MIPs are favoured by a moderate initiator concentration, ie, initiator:total monomer (I:TM) ratio of 1:131, while low I:TM ratio (ie, 1:200) drastically reduced template incorporation and binding capacity. Vigorous agitation by stirring showed higher template incorporation but significantly lower template rebinding compared to that prepared without agitation. While the imprinting efficiencies for the best performing bulk and precipitation TAU MIPs generated in this study were moderate, 41% and 60%, respectively, their rebinding capacities were only between 3 and 4% of the incorporated template. We also present quantitative nuclear magnetic resonance spectroscopy as an efficient method for MIP characterisation.

KEYWORDS

2,6-bis(acrylamido)pyridine, donor-acceptor-donor hydrogen bond array, molecularly imprinted polymers, precipitation imprinting, precipitation polymerisation, quantitative NMR

1 | INTRODUCTION

Molecularly imprinted polymers or MIPs are robust, porous polymeric molecular moulds with recognition capabilities specific for its target molecule. The most common approach to molecular imprinting is by the self-assembly (or non-covalent) method. To create the molecular

imprints by this method, a template T (usually the target molecule or an analogue), is allowed to associate with a functional monomer FM, by virtue of their complementary functional groups, in solution. The FM is selected such that it interacts strongly with the template forming a stable T:FM cluster in the pre-polymer mix. These T:FM clusters are fixed in place, in a three-dimensional framework, by the polymerisation reaction of the FM with an excess of di (or tri) polymerisable molecule, ie, the crosslinker XL. Once the template/target is removed from the solid polymers, it leaves a cavity (a mould) that is complementary in shape and functionality

This article is published in Journal of Molecular Recognition as part of the Special Issue 'MIP2016 The 9th International Conference on Molecular Imprinting, edited by David Spivak, Department of Chemistry, Louisiana State University, Baton Rouge, Louisiana'.

with the template/target and, therefore, capable of recognising and selectively rebinding the template.

Molecular imprinting proved to be efficient using commercially available functional monomers capable of forming strong interactions with the template/target. However, a number of acylamido-pyridine¹⁻⁵ and pyrimidine-based⁶ functional monomers have been specifically designed for templates/targets containing an imide group that can form an array of hydrogen bonding interactions⁷ (Figure 1) with these amide-based monomers affording high affinity binding sites.^{8,9} One of the widely studied custom-designed pyrimidine-based functional monomer is the 2,6-bis-(acrylamido)pyridine (BAAPy, **1**, Figure 2), which has been widely explored in imprinting imide-containing templates, such as fluorouracil,⁴ cyclobarbital,¹⁰ and barbiturates.¹¹ Due to the displayed specificity of the BAAPy-synthesised MIPs towards small molecules, researchers moved to using more complex and bulkier templates like riboflavin,² glutamic acid,¹² and uracil derivatives.^{5,6} In a more recent study, the application of BAAPy in the imprinting process of a more complex uracil-containing compound, nucleosides, was proven to be efficient in bulk format. 2′3′5′-Tri-O-acyl uridines, with different alkyl chain lengths (attached to the ribose ring), were used as dummy templates for the recognition of uridine nucleosides. Among

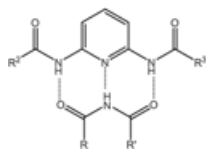


FIGURE 1 Illustration of the DAD/ADA hydrogen bonding array of the trans-amide group of a bis-acrylamidopyridine-based compound and an imide functionality

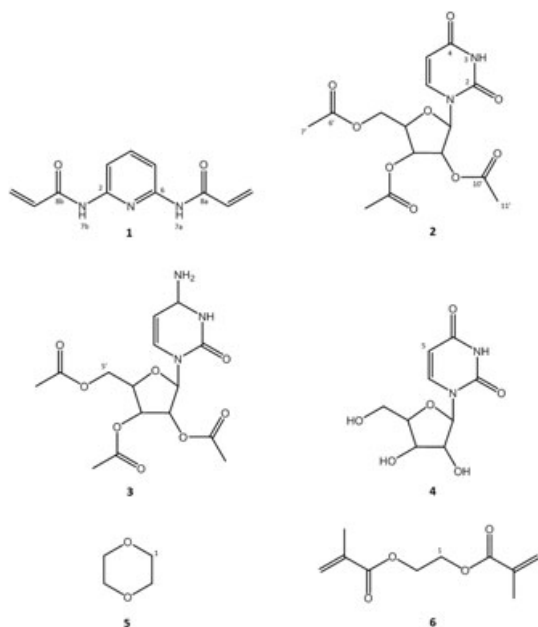


FIGURE 2 2,6-Bis(acrylamido)pyridine, BAAPy (**1**), 2′3′5′-tri-O-acetyluridine, TAU (**2**), 2′3′5′-tri-O-acetylcytidine (**3**), uridine (**4**), dioxane (**5**), and ethylene glycol dimethacrylate (**6**). Labelled atoms correspond to nuclei used for NMR analysis

the tested systems, the MIP for 2′,3′,5′-tri-O-acetyl uridine (TAU) showed higher binding capacity, selectivity, and specificity than the other tested templates as determined by frontal chromatography.⁵

Herein, we present a detailed assessment of the imprinting efficiency and binding performance of TAU MIPs prepared by precipitation polymerisation using BAAPy as functional monomer which, to the best of our knowledge, have not yet been fully investigated. As an added value to this study, we also present the application of quantitative nuclear magnetic resonance spectroscopy (qNMR) for polymer composition and in situ binding measurements. We found that the stoichiometric 1:1 T:FM ratio has not been maintained in precipitation polymerisation and a TAU:BAAPy ratio of 1:2.5 was obtained for MIP microspheres prepared in acetonitrile without agitation. This precipitation MIP afforded an affinity constant and binding capacity higher than its bulk counterpart. Molecular modelling, NMR studies, and selectivity assays indicate that, aside from the DAD/ADA hydrogen bond interaction, BAAPy also interacts with the acetyl groups of TAU. Imprinting efficiency (ie, template incorporation) and binding capacity of precipitation MIPs have also been shown to be affected by the initiator concentration and method of agitation.

2 | EXPERIMENTAL

2.1 | Materials and reagents

BAAPy (**1**) was initially provided by Dr. Andrew Hall and later synthesised according to a standard procedure¹¹ briefly described below. 2,6-Diaminopyridine, acryloyl chloride, and triethylamine were purchased from Sigma-Aldrich and were used as received. Ethylene glycol dimethacrylate (EGDMA, Sigma-Aldrich) was purified by passing through a basic aluminium oxide column. TAU (**2**, Sigma-Aldrich) was used as received. 2′3′5′-tri-O-Acetylcytidine (TAC, **3**) was obtained by neutralising acetylcytidine hydrochloride (Sigma-Aldrich) with NaHCO₃, extracted in dichloromethane and dried in vacuo. Uridine (**4**, Sigma-Aldrich) was recrystallised from methanol prior to use. 2,2′-Azobisisobutyronitrile (AIBN, Dupont Chemicals) was recrystallised from methanol prior to use. 1,4-Dioxane was purchased from Acros and used as received. DMSO-*d*₆ was purchased from Cambridge Laboratories. Acetonitrile, methanol, chloroform, and diethyl ether (VWR Chemicals) were of analytical grade and used as received.

2.2 | Synthesis of 2,6-bis(acrylamido)pyridine (BAAPy)

BAAPy was synthesised according to the procedure of Yano et al.⁷ 2,6-Diaminopyridine (5.46 g, 50 mmol) and triethylamine (16.7 mL, 120 mmol) were dissolved in 150 mL of chloroform and chilled and stirred at 0°C. Acryloyl chloride (9.73 mL, 120 mmol) was added dropwise to the stirred solution and maintained in an ice-bath until all acryloyl chloride has been added. The reaction mixture was stirred for a further 12 hours at room temperature. The solvent was removed in vacuo, and the residue was dissolved in 200 mL of methanol then poured onto 1.6 L of deionised water, with stirring, to precipitate the BAAPy product. The precipitate was collected, dried in a vacuum oven at 40°C, and afforded

1.23 g, ~30%. (^1H NMR, DMSO- d_6); 5.80 and 6.32 ppm ($-\text{C}=\text{CH}_2$), 6.67 ppm (vinyllic $-\text{C}=\text{CH}-$), 8.22 ($-\text{C}=\text{CH}-$ of the pyridine ring) and 10.31 ppm (NH).

2.3 | TAU-BAAPy interaction studies

Molecular modelling simulation software Spartan '04 (Wavefunction, Inc. USA) was employed. ^1H and ^{13}C NMR titration experiments were conducted using Bruker Avance III 600 MHz-NMR on a 5-mm probe at 30°C and 60°C and processed using Bruker Topspin 3.2 software. Increasing amount of BAAPy (from a 50.0 mM in acetonitrile) ranging from 1.00 to 10.00 mmol in 20.0 μL (1.00 mmol) increments was added to 1.00 μmol (370.31 μg) of TAU in 0.50 mL of acetonitrile. *d*-DMSO was used as a lock and placed in a co-axial insert. The complexation-induced shifts of the carbons and the protons of both BAAPy and TAU were observed.

2.4 | Synthesis of molecularly imprinted polymers

For precipitation imprinting, TAU imprinted polymers were synthesised in acetonitrile and chloroform at 1:1:20 TAU:BAAPy:EGDMA (T:FM:XL) feed ratio. The polymerisation mixture was prepared by dissolving 23.8 μmol (198.8 mg) TAU, 23.8 μmol (5.170 mg) of BAAPy, and 476.1 μmol (94.0 mg, 90 μL) of EGDMA with the desired amount of AIBN initiator in 5.00 mL of acetonitrile, ie, 0.500 mmol total monomers in 5.00-mL acetonitrile (20-mg total monomers per mL acetonitrile). After purging with nitrogen gas for 15 minutes, the reaction mixture was polymerised for 24 hours in a water bath (Julabo F12-ED Refrigerated/Heating Circulator) at 60°C. Once the reaction is complete, the microspheres were separated from the post polymerisation solution by centrifugation for 20 minutes at 2500 rpm, and the post polymerisation solutions were stored for NMR analyses. Subsequently, the template was removed by stirring the collected microspheres with approximately 3 mL of methanol:acetic acid solution (90:10) overnight, washing 3 \times with 3 mL methanol, then a further 1 mL of methanol for NMR analysis. This extraction procedure was repeated until no template was detected in the centrifugate by ^1H NMR. The microspheres were then washed with diethyl ether and placed in a vacuum oven at 40°C for further drying. Monoliths were synthesised following Krstulja, et al's⁵ formulation of 1:1:20 TAU:BAAPy:EGDMA (T:FM:XL) ratio. 537.0 μmol (198.8 mg) of TAU, 537.0 μmol (116.6 mg) of BAAPy, 10.7 mmol (2.05 mL) of EGDMA, and 85.9 μmol (14.11 mg) of AIBN as initiator were dissolved in 3.00 mL (3 mL/11.24 mmol total monomers) of chloroform or acetonitrile as porogens. After purging with nitrogen gas for 15 minutes, the reaction mixtures were polymerised for 24 hours at 60°C. The resulting monolithic products were incubated with 5.0 mL of the porogen for 24 hours without agitation, after which the solution was subjected to ^1H NMR analysis. Monoliths were crushed and sieved to sizes between 32 and 45 μm . Template removal followed the same procedure as with the microspheres. Non-imprinted polymers (NIPs) for both precipitation and bulk polymerisation process were produced in exactly same formulations and conditions as with the imprinted polymers in the absence of the template. Both MIPs and NIPs for all formulations were synthesised in triplicates.

2.5 | Determination of polymer composition and template incorporation

Polymer composition and template incorporation were determined by calculating the amounts of left-over monomers and template in solution, post-polymerisation, by ^1H NMR on a 600-MHz Bruker Avance III. 500 μL of the filtered reaction mixture was placed in a 5-mm probe, while 500- μL 1,4-dioxane, **5** (the reference standard) in DMSO- d_6 was enclosed in a coaxial insert. Spectra of both the initial and the post polymerisation solutions were acquired and processed using Bruker Topspin 3.2 software. An example of a ^1H NMR spectrum is shown in Figure S1 (ESI) together with the peak assignments used for quantitation. Calibration curves (eg, ESI Figure S2) were prepared using the following peaks: $\text{O}-\text{CH}_2-$ (H1 of **6**, ie, **6-1**, 4.68 ppm) for EGDMA, $-\text{CH}=\text{CH}-$ (**2-5**, 6.22 ppm) for TAU, and $\text{CH}-\text{CH}=\text{}$ (**1-3**, 8.25 ppm) for BAAPy. These peaks were chosen because they do not overlap with the acetonitrile solvent peak at ~2.7 ppm ensuring flat baseline and accurate integration in this region.

2.6 | Template rebinding studies

Time-binding experiments were conducted in situ by ^1H NMR at 35°C by incubating 10.0 mg of polymer PP-1:1-A (both NIP and MIP) in 0.50 mL of 50.0 μM TAU in acetonitrile in a 5-mm NMR tube at various times from 15 to 180 minutes. The amount of TAU remaining in solution (without separating the microspheres) was quantified by monitoring the peak at 6.22 ppm corresponding to proton 5 of TAU (**2-5**) with respect to the peak at 3.57 ppm of 100 μM 1,4-dioxane in DMSO-*d* internal standard contained in a co-axial insert. These peaks were chosen because they do not overlap with the acetonitrile solvent peak at ~2.7 ppm.

For subsequent batch rebinding experiments, 10.0 mg of polymers was incubated (with shaking) in 0.500 mL of 100 μM TAU rebinding solution in acetonitrile in 5-mm NMR tubes and shaken (Intelli mixer RM-2) for 1 hour. The suspensions were then subjected to NMR analyses as with the time binding experiments. Binding isotherms were obtained for PP-1-A and BP-1-A by incubating the polymers at various concentrations of TAU ranging from 1 to 100 μM . Post-rebinding solutions were collected after centrifugation and filtration (necessary especially for low TAU concentrations) prior to ^1H NMR as with the time binding experiments.

2.7 | Selectivity studies

The affinity of the TAU-imprinted microspheres towards the two analogues: TAC (**3**) and uridine (**4**) was tested using PP-1-A by incubating 10.0 mg of polymers in 0.500 mL of 50 μM solution of **3** or **4** in 5-mm NMR tubes and shaken for 1 hour. The suspensions were then subjected to in situ NMR analyses using 10 μM 1,4-dioxane internal standard by monitoring the 4.137 (H5') and 6.077 (H5) ppm peaks for **3** and **4**, respectively. Selectivity of the TAU-imprinted microspheres against TAC was tested using PP-1-A by incubating 10.0 mg of polymers in a mixed solution of 0.250 mL of 50 μM solution of TAU and 0.250 mL of 50 μM solution of TAC in 5-mm NMR tubes and shaken for 1 hour. The suspensions were then subjected to in situ NMR analyses as with the non-

competitive affinity tests. The procedure was repeated using 0.250 mL of 50 μ M solution of TAU and 0.250 mL of 50 μ M solution of uridine.

2.8 | Sample morphology

Scanning electron microscopy (SEM) imaging was conducted using a Zeiss SEM Gemini instrument. Dried microspheres were gold coated thrice using an SPI-Module sputter coater: twice in 45° angle and once lying flat, prior to SEM imaging. Images of the particles were obtained using a magnification of 10 000–30 000, and were analysed using Zeiss Zen lite 2012 software.

2.9 | Particle size analyses

Dynamic light scattering (DLS) measurements were carried out using a Malvern Zetasizer Nano ZS with DTS Version 5.03 a software package (Malvern Instruments Ltd., Worcestershire, UK). Approximately 0.1 mg of the sample was suspended in ~0.5 mL of acetonitrile and sonicated using a benchtop ultrasonicator for 10 s to minimise aggregation of particles. Three measurements were carried out for each sample, and average sizes are expressed in terms of intensity weighted size distributions based on hydrodynamic diameters (d_H).

3 | RESULTS AND DISCUSSION

BAAPy as a functional monomer in bulk imprinting of uracil derivatives with variable acyl group chain lengths has been explored by the group of Krstulja et al.^{4,5} They investigated uracil-based targets, and TAU (2) imprinted MIPs have been shown to exhibit the highest affinity (number of TAU binding sites = 3.42 μ mol/g, $K_a = 1.7 \times 10^4$ L/mol) and selectivity. While BAAPy has been extensively used in bulk imprinting, its utility in precipitation polymerisation has been limited. There has only been one report on BAAPy-based microspheres for solid phase extraction of barbiturates in human urine samples.¹³ This current study evaluates the performance of BAAPy as a functional monomer in precipitation imprinting of TAU, particularly monitoring both imprinting and binding efficiencies.

3.1 | Synthesis of MIPs

3.1.1 | Bulk polymerisation

TAU MIPs were first synthesised by bulk polymerisation using the 1:1:20 TAU:BAAPy:EGDMA formulation of Krstulja, et al.⁵ but employing AIBN, instead of azo-bis-dimethylvaleronitrile (ABDV), at 60°C using chloroform (BP-1:1-C) and acetonitrile (BP-1:1-A) as porogens. Krstulja et al have shown chloroform as an efficient porogen in bulk polymerisation, but we were also keen to use acetonitrile to be able to compare with precipitation MIPs also generated in acetonitrile. TAU was reported to exhibit comparable solubility in both solvents (≥ 100 mM).⁵ The polymers obtained from both acetonitrile (BP-1:1-A) and chloroform (BP-1:1-C) are highly porous (ESI Figure S3). While microspheres seem to be formed at the surface

of the MIPs, both MIPs and NIPs generally showed bulk morphology expected from bulk molecular imprinting process in the presence of limited amount of porogen.

The composition of MIPs and NIPs was determined indirectly by calculating the amounts of left-over (unpolymerised) monomers and template in solution post-polymerisation with respect to the pre-polymerisation mixture by ¹H NMR spectroscopy. The results, summarised in Tables 1 and S1 (ESI), show high conversions for EGDMA ($\geq 95\%$) and BAAPy ($\geq 92\%$) in the NIPs resulting in FM:XL mol ratios of 1:20 (BP-1:1-A) and 1:21 (BP-1:1-C) approximating the feed formulation of 1:20. The BAAPy conversion in the MIPs, on the other hand, was slightly lower at 64% and 77% for chloroform and acetonitrile-porogenated MIPs, respectively, while the EGDMA conversion remains high (94%) and comparable to that of the NIPs, resulting in FM:XL mol ratios of 1:29 and 1:25, respectively. Nevertheless, TAU incorporation within the polymers while moderate, 143 ± 1 μ mol/g (60%) and 158 ± 5 μ mol/g (66%) for BP-1:1-C and BP-1:1-A, respectively, with respect to the TAU feed (240 μ mol/g), afforded T:FM ratios of 0.9:1 and 0.8:1, respectively, approximating the expected 1:1 stoichiometric T:FM relationship also obtained by Krstulja, et al.⁵ We surmised that the lower BAAPy conversion in the MIPs is due to the formation of the TAU:BAAPy complex which is less soluble in the porogen than the uncomplexed TAU and BAAPy. Turbidity tests confirmed our hypothesis. We observed a decrease in transmittance (from 98% to as low as 40% between 400 and 700 nm) upon the addition of TAU to a BAAPy solution in acetonitrile and chloroform indicating formation of less soluble species.

3.1.2 | Precipitation polymerisation

TAU MIPs (PP-1:1-A) were subsequently synthesised by precipitation polymerisation following the bulk formulation with chloroform and acetonitrile (10 mL per mmol monomer) as porogens. Polymers prepared in chloroform and even with 50% chloroform/50% acetonitrile by volume resulted in gels^{14–16} so only PP-1:1-A was subjected to further characterisation. As shown in Figure 3, PP-1:1-A are spherical particles with average hydrodynamic sizes (d_H) of 337 and 368 nm for MIP and NIP, respectively, as measured by DLS. Particle aggregation is evident from SEM images which is consistent with their broad PDIs (~0.8).

As with bulk imprinting, the FM:XL ratio in the PP-1:1-A feed was kept at 1:20. However, the conversion of EGDMA was lower (ESI Table S1), ie, ~80%, while that of BAAPy higher (~90%), than what was observed in BP polymers resulting in a higher BAAPy:EGDMA ratio of 1:18 for NIP and 1:16 for MIP (Table 1). Unlike the bulk process, we did not observe precipitation of the TAU:BAAPy complex (as indicated by a decrease in solution transmittance) and we presume that the degree of BAAPy and EGDMA conversions is a function of their copolymerisation tendencies. Interestingly, the TAU:BAAPy ratio obtained was 1:2.5 (ie, 0.4:1) as only 98 ± 1 μ mol/g (41%) was incorporated, a deviation from the 1:1 stoichiometric relationship obtained with bulk MIPs and expected from BAAPy-based uracil MIPs. Our results seem to

TABLE 1 TAU imprinting results for bulk (BP) and precipitation (PP) polymers

Polymers ^a		TAU:BAAPy:EGDMA mole ratios ^b		Particle size, nm (PDI)	TAU ^c , $\mu\text{mol/g}^d$		IF ^e
		Feed	Polymer		Imprinted	Rebound	
BP-1:1-A	MIPs	1:1:20	0.78: 1: 25	32–45 μm	158 \pm 5	3.57 \pm 0.11	2.0
	NIPs		1:20			1.81 \pm 0.18	
BP-1:1-C	MIPs	1:1:20	0.86: 1: 29		143 \pm 1	4.07 \pm 0.2	1.7
	NIPs		1:21			2.39 \pm 0.1	
PP-1:1-A	MIPs	1:1:20	0.4:1:16	337 \pm 1 (0.774)	98 \pm 2	3.64 \pm 0.03	3.0
	NIPs		1:18	368 \pm 2 (0.794)		1.23 \pm 0.02	
PP-1:1-A-St ^f	MIPs	1:1:20	0.84: 1: 22	Not measured	173 \pm 3	0.29 \pm 0.02	1.5
	NIPs		1:19			0.20 \pm 0.01	
PP-1:1-A-Rd ^g	MIPs	1:1:20	0.58: 1: 18	Not measured	153 \pm 4	1.22 \pm 0.10	1.4
	NIPs		1:23			0.86 \pm 0.10	
PP-1:1-A-150 ^h	MIPs	1:1:20	0.29: 1: 19	387 \pm 1 (0.374)	73 \pm 2	1.14 \pm 0.10	2.1
	NIPs		1:20	490 \pm 1 (0.507)		0.54 \pm 0.01	
PP-1:1-A-1200 ⁱ	MIPs	1:1:20	0.16:1:20	468 \pm 1 (0.716)	38 \pm 2	0.56 \pm 0.01	1.2
	NIPs		1:21	380 \pm 1 (0.417)		0.46 \pm 0.03	

^aA = acetonitrile, C = chloroform.

^bOnly FM:XL for NIPs.

^cTAU in feed = 240 $\mu\text{mol/g}$ except for PP-2:1-A = 480 $\mu\text{mol/g}$.

^d $\mu\text{mol/g}$ = $\mu\text{mol template/g total monomers}$.

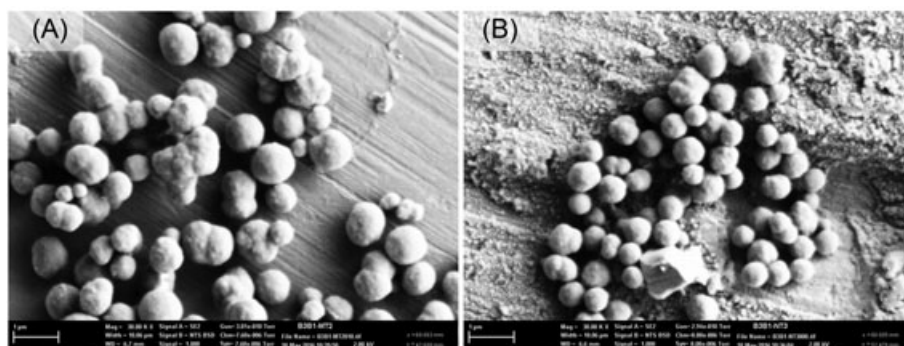
^eImprinting factor = bound MIP/bound NIP.

^fSt = stirred.

^gRd = rolled.

^hInitiator:total monomer (BAAPy + EGDMA) mol ratio = 1:50.

ⁱInitiator:total monomer ratio = 1:200; Note: Initiator:total monomer ratio of all other polymers = 1:131.

**FIGURE 3** SEM images of precipitation polymers PP-1:1-A MIP (A) and NIP (B)

suggest that template-monomer interaction is influenced and can be optimised by solvent dilution. Beijer et al have extensively studied the interaction of BAAPy with uracil derivatives and have shown that the DAD H-bond induced 1:1 complex only prevail if no other functional group or interaction sites other than the imide is present.¹⁷ TAU, on the other hand, has three ester functionalities surrounding the ribose ring which can be possible points of interaction with BAAPy. Evidence to this effect was obtained from ¹H NMR titration and molecular modelling template-monomer interaction studies.

3.2 | TAU-BAAPy interaction studies

The computer generated 1:1 TAU:BAAPy complex (Spartan '14 v1.1.8) given in Figure 4A shows the ADA/DAD H-bonding interactions to be the predominant with distances between the interacting atoms of 1.8 Å.¹⁸ Nevertheless, while these H-bonding arrays are still evident when the TAU:BAAPy ratio is decreased to 1:3, mimicking the PP-1:1-A system, the amido protons of the other two BAAPy units have also been observed to interact with the carbonyl oxygen 6' and 10' of TAU (Figure 4B). The distances between the ADA/DAD H-bond

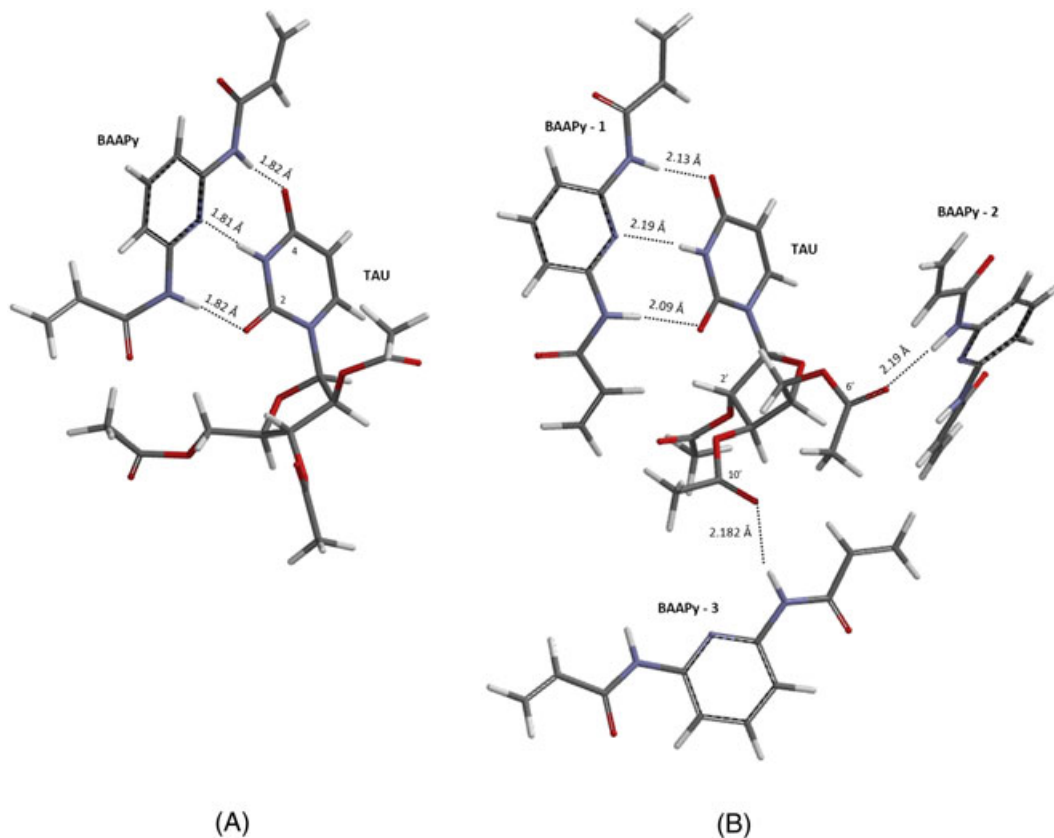


FIGURE 4 The predominant hydrogen bonding interaction points (distances $2.2 \geq 2.5 \text{ \AA}$) between BAAPy and TAU measured by Spartan '14 v1.1.8 in a 1:1 (A) and 1:3 (B) TAU:BAAPy clusters

interacting atoms have also been shown to slightly increase to 2.1–2.2 \AA , suggesting weaker interactions than with the 1:1 ratio, but this has been compensated by the formation of two additional H-bond interactions with two other BAAPy units.

To verify the interactions observed from molecular modelling, ^1H and ^{13}C NMR titration experiments were carried out in acetonitrile (the porogen) at 60°C (the reaction temperature) monitoring movements in chemical shifts (≥ 0.2 ppm) of protons and carbons, respectively, brought about by interactions between BAAPy and TAU. Representative ^1H and ^{13}C NMR spectra showing peak shifts of interacting nuclei are given in ESI Figures S4 and S5, respectively. These peak movements are also illustrated in Figures 5 and S6 (ESI).

The DAD/ADA hydrogen bond array interactions between the imide group of TAU and the amide group of BAAPy are evident from the chemical shift movements of the amido protons (Figure 5). The H-bond donating amido proton of TAU (2-3, see Figure 2 for proton/carbon assignments) showed a marked upfield peak movement presumably upon interaction with the H-bond acceptor nitrogen (1-1) of BAAPy. Conversely, the amido protons of BAAPy (1-7a,b) experienced a downfield chemical shift movement in the presence of TAU attributed to enhanced deshielding by amido oxygens 2-2 and 2-4 of TAU. Consequently, carbons 2-2 and 2-4 would have been more shielded and thus underwent a shift upfield (ESI, Figure S6).

The chemical shift movements of other carbon nuclei (ESI, Figure S6) indicate additional interactions between TAU and BAAPy aside from the DAD/ADA H-bonding array. In particular, TAU acyl carbons 6' and 10' (2-6' and 2-10') as well as their adjacent methyl groups

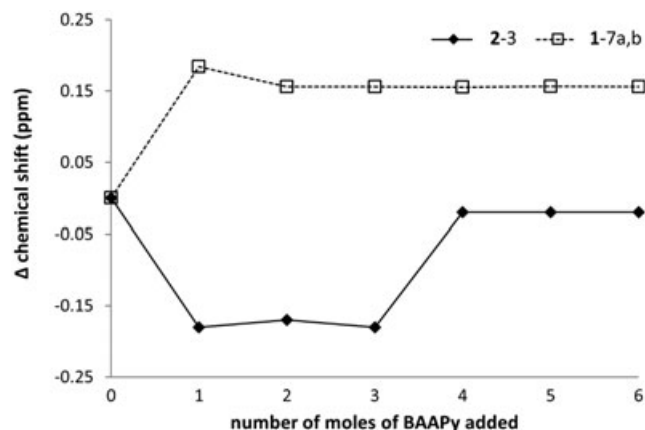


FIGURE 5 Chemical shifts of the imido protons of TAU (2-3) and BAAPy (1-7a,b) measured by ^1H NMR in acetonitrile at 60°C . Note that chemical shift = chemical shift of the mixture – chemical shift of the pure solution of TAU or BAAPy. *d*-DMSO used for locking was contained in a co-axial insert

2-7' and 2-11', respectively, exhibited upfield shifts which could be attributed to additional shielding brought about by the interaction of the acyl oxygens with the amido proton of BAAPy. These interactions are evident in the computer image generated for the 1:3 TAU:BAAPy complex. The carbons 1-8a,b of BAAPy also showed movements indicating interactions of the amido oxygens with, most possibly, the amino hydrogen of TAU or its own. We have certainly observed from

molecular modelling that, at $\geq 1:4$ TAU:BAAPy ratios, intra-BAAPy interactions predominate consistent with the ^1H NMR titration results, which show negligible peak movement of the TAU amido nitrogen at 1:5 TAU:BAAPy ratio. It would seem that BAAPy carbons 1-2,6 also experienced the deshielding of the adjacent amido hydrogens by the 2-2 and 2-4 amido oxygens causing an downfield peak movement at 1:1 TAU:BAAPy stoichiometry. However, at lower TAU:BAAPy ratios (ie, $\geq 1:2$), the peaks reversed to upfield shifts indicating a change in electron density in their proximity. This suggests that at 1:1 stoichiometric ratio, the DAD/ADA H-bonding array is the predominant interaction between TAU and BAAPy and that BAAPy participates in other interactions at lower TAU:BAAPy ratios.

3.3 | Rebinding studies

Krstulja et al⁵ reported the binding performance of TAU bulk MIPs using frontal chromatography and recorded high imprinting factors (IF = 48) based on the difference of retention factors between MIP and NIP. For this study, we opted to use batch binding assays and developed an *in situ* quantitative solution ^1H NMR protocol to measure the unbound TAU left in solution, as with HPLC, without the need to separate the polymeric particles. Employing 1,4-dioxane as a reference standard, this *in situ* method was applied to rebinding tests at analyte concentration of $\geq 10\mu\text{M}$ giving results that are comparable to the conventional method that involves separation of polymer particles prior to measurements. TAU rebinding tests were first conducted to determine the optimum TAU rebinding time using PP-1:1-A. Maximum binding capacity was achieved after 60 minutes (ESI Figure S7); therefore, subsequent binding assays were measured after 60 minutes of incubation and an additional 15 minutes of test sample preparation.

3.3.1 | TAU rebinding efficiency

Figure 6 gives the rebinding results for bulk (BP-1:1-A and BP-1:1-A) and precipitation (PP-1:1-A) polymers after 1 hour of incubation. As earlier presented in Table 1, 64% and 77% of the TAU added in the feed formulation of chloroform and acetonitrile-porogenated MIPs, respectively, were incorporated in the monolithic MIPs resulting in a 1:1 stoichiometric T:FM ratio, but only rebound

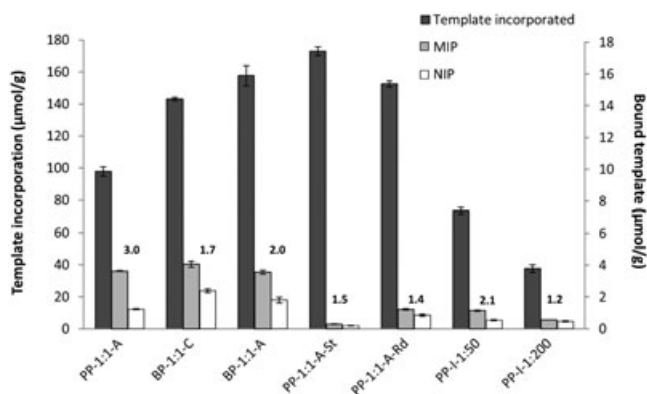


FIGURE 6 TAU incorporation and binding efficiencies of bulk polymers and precipitation polymers. 10.0 mg of polymers was incubated in 0.500 mL of 100 μM TAU solution for 1 h prior to quantitative ^1H NMR analysis

2.8% ($4.1 \pm 0.2 \mu\text{mol/g}$) and 2.3% ($3.6 \pm 0.1 \mu\text{mol/g}$) of it, respectively. These results suggest that most of the incorporated template was not converted to high fidelity imprints in bulk imprinting, with some possibly destroyed during grinding of the monoliths.¹⁹⁻²⁶ Conversely, their respective NIPs also recorded comparable TAU binding of $2.4 \pm 0.1 \mu\text{mol/g}$ (BP-1:1-C) and $1.8 \pm 0.2 \mu\text{mol/g}$ (BP-1:1-A) giving imprinting factors of 1.7 and 2.0, respectively.

In contrast to the BP polymers, PP-1:1-A only incorporated 41% ($98 \mu\text{mol/g}$) of the TAU feed resulting in a 1:2.5 TAU:BAAPy ratio in the polymer, rather than 1:1. As presented in the previous section, both molecular modelling and NMR titration experiments support formation of 1:3 TAU:BAAPy complexes due to the presence of the acyl groups in TAU, in addition to its imide functionality, capable of interacting with the amido proton of BAAPy. Nevertheless, PP-1:1-A MIP managed to rebound 3.7% ($3.64 \pm 0.03 \mu\text{mol/g}$) of the imprinted TAU, 1.5 times higher than that of BP-1:1-A (2.4%). These results suggest that imprinting is more efficient by precipitation polymerisation than by bulk.^{27,28} In the case of the non-imprinted polymers, PP-1:1-A NIP gave a TAU binding ($1.23 \pm 0.02 \mu\text{mol/g}$) 1.5 times lower than that of BP-1:1-A NIP ($1.81 \pm 0.18 \mu\text{mol/g}$) resulting in an imprinting factor of 3.0, higher than that of BP-1:1-A (ie, 2.0).

3.3.2 | Characterisation of binding sites: binding isotherms

Binding isotherms for PP-1:1-A and its bulk counterpart BP-1:1-A are presented in Figure 7 together with the binding parameters K (binding affinity constant) and N (total number of binding sites) derived from non-linear (NL) Langmuir curves. As an expected consequence of molecular imprinting, both BP and PP MIPs showed higher TAU binding and total binding sites (N) than their non-imprinted counterparts. Likewise, K for MIPs are also higher than that for NIPs indicating that higher affinity binding sites for TAU were created during molecular imprinting.

Krstulja et al⁵ have reported K values an order of magnitude lower than the values we obtained ($1.2 \times 10^3 \text{ M}^{-1}$ and $0.3 \times 10^3 \text{ M}^{-1}$ for MIP and NIP, respectively) for a TAU/BAAPy system equivalent to our BP polymers also analysed using the NL model and comparable concentration range ($\leq 100\mu\text{M}$). Nevertheless, both calculations recorded a K_{MIP} 4 times higher than the corresponding K_{NIP} confirming efficient imprinting of TAU in both cases. In the case of N , Krstulja et al obtained values twice as high as ours, $10.65 \mu\text{mol/g}$ vs $4.54 \mu\text{mol/g}$ for MIP and $4.88 \mu\text{mol/g}$ vs $3.34 \mu\text{mol/g}$ for NIP, and a higher $N_{\text{MIP}}/N_{\text{NIP}}$ ratio of 2.2 compared to only 1.4 in this study. It is noteworthy that Krstulja et al generated their polymers at a temperature of 40°C (vs 60°C in this present study) and have employed frontal chromatography for binding calculations which could account for the difference in K and N values obtained by the two studies.

Our results also showed the K for PP MIP ($7.5 \pm 0.8 \times 10^4 \text{ M}^{-1}$) to be 2 times higher than that for BP MIP ($3.4 \pm 0.3 \times 10^4 \text{ M}^{-1}$) and 10 times higher than its corresponding NIP. Conversely, N for PP MIP ($5.60 \pm 0.39 \mu\text{mol/g}$) is slightly higher than that for its bulk counterpart ($4.54 \pm 0.22 \mu\text{mol/g}$) and twice as much as the N of its corresponding BP-NIP. Both PP and BP NIPs afforded comparable K 's and N 's. These results indicate that precipitation polymerisation was able to generate higher affinity binding sites for TAU which could be attributed to a

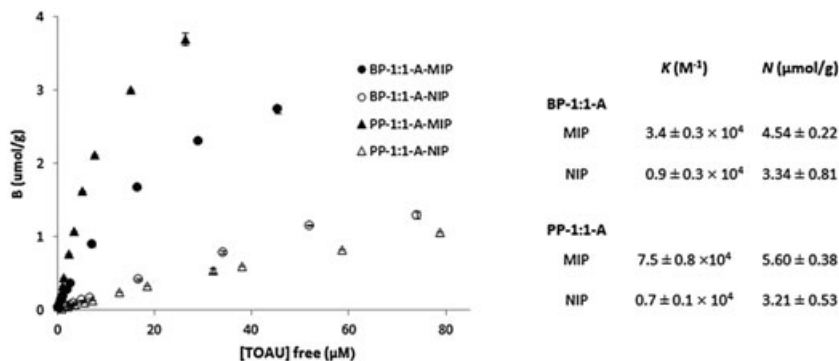


FIGURE 7 Binding isotherms of BP-1:1-A and PP-1:1-A polymers. Isotherms obtained using 10-mg polymer incubated for 1 h in 0.500 mL of 1 to 100 μM TAU solution. Free TAU was measured by in situ quantitative ^1H NMR spectroscopy. Binding affinity constants (K) and number of binding sites were estimated from Prism GraphPad using the one-site hyperbola model. Errors are at 95% confidence level

stronger T:FM interaction provided by a maximal interaction by virtue of the 1:2.5 TAU:BAAPy ratio. Previous studies^{23,29} have also demonstrated that precipitation polymerisation yields more homogenous and higher affinity constants imprinted polymers compared to bulk polymerisation.

3.4 | Selectivity studies

PP-1:1-A have been shown to possess higher affinity binding sites than its bulk counterpart while showing a non-stoichiometric TAU:BAAPy ratio of 1:2.5. Molecular modelling and NMR studies conducted on this system suggest favourable interactions, other than the DAD/ADA H-bond array, involving the acetyl groups in the ribose ring of TAU. Thus, selectivity studies for PP-1:1-A were conducted against analogues 2,3,5-tri-*O*-acetyl cytidine, TAC (3) and uridine, Ur (4) (see Figure 2 for structures). Unlike TAU, uridine does not have the three acetyl groups in the ribose ring, while TAC does possess the three acetyl groups in the ribose ring but not the imide group.

Results of the non-competitive cross-binding assays on PP-1:1-A MIP are given in Figure 8. While the template TAU was rebound at $3.64 \pm 0.03 \mu\text{mol/g}$, only $2.50 \pm 0.01 \mu\text{mol/g}$ of uridine was bound

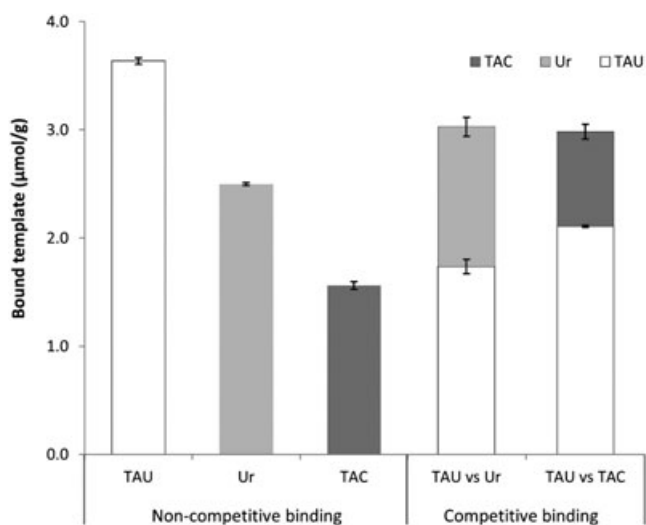


FIGURE 8 Binding capacities of PP-1:1-A MIP in non-competitive cross-binding and competitive assays against uridine (Ur) and 2',3',5'-tri-*O*-acetyl-cytidine (TAC). 10.0 mg of polymers was incubated for 1 h prior to ^1H NMR analysis using 0.500 mL of 100 μM of analyte for non-competitive rebounding and equimolar concentration (50 μM) of TAU and analogue for competitive rebounding

decreasing to $1.56 \pm 0.03 \mu\text{mol/g}$ with TAC. Similarly, in competitive binding assays, while the total bound quantities of TAU + uridine and TAU + TAC mixtures are comparable, less TAC was bound than uridine ($0.91 \pm 0.07 \mu\text{mol/g}$ vs $1.33 \pm 0.09 \mu\text{mol/g}$). These results indicate that analyte binding is predominantly governed by the DAD/ADA hydrogen bond as shown by the significant amount of bound uridine compared to the non-imide containing TAC. Nevertheless, binding of uridine under non-competitive condition is 30% lower than TAU suggesting that the interaction of BAAPy with the acetyl groups in the ribose ring of TAU (not found in uridine) also enhances TAU binding. Further, even with the disruption of the DAD/ADA hydrogen bonding array, TAC still registered a moderate binding of 43% (non-competitive) and 23% (competitive) with respect to TAU suggesting the importance of the acetyl groups in the ribose ring. It is noteworthy that the amino group of TAC could also interact with BAAPy and could also be responsible for some of its binding.

We subjected the two analogues to molecular modelling calculations, using the previously generated 1:3 TAU:BAAPy cluster presented in Figure 4B, by “freezing” the 3 BAAPy units in place and replacing TAU with either uridine or TAC. We found that uridine interacts with one BAAPy unit via the DAD/ADA hydrogen bonding array (ESI Figure S8A), and no interaction was observed with the other two BAAPy units which, with TAU, showed interactions with the acetyl groups in the ribose ring. With TAC (ESI Figure S8B), interaction was evident between BAAPy units 2 and 3 and the acetyl groups of TAC, similar to what was observed with TAU. BAAPy unit 1 also interacted with the amino group of TAC but the DAD/ADA hydrogen bond array of interaction was not maintained. These molecular modelling results are consistent with the cross- and competitive binding analyses.

3.5 | Effect of initiator concentration

Mijangos et al.^{30,31} have compared the effects of the amount of the initiator [1,1'-azobis(cyclohexane-1-carbonitrile)] in the bulk imprinting of (+)-ephedrine at 80°C and found that, apart from its effect on polymer rigidity, imprinted polymers produced in lower amount of initiator (1%, initiator:total monomer (I:TM) ratio = 1:267) performed better than the MIPs produced in higher amount of initiator (5%, I:TM ratio = 1:1335). They hypothesised that the heat of reaction, brought about by high amount of the initiator in the feed, disrupts the complex formation between the template and the functional monomer reducing the affinity and selectivity of the MIPs.

In this study, PP-1:1-A, prepared with I:TM ratio of 1:131 following published formulation,⁵ was compared with two other TAU precipitation MIP systems prepared with I:TM ratios of 1:50 (PP-I-1:50) and 1:200 (PP-I-1:200) using the same formulation and porogen as PP-1:1-A. Yang et al observed that higher concentration of initiator resulted in bigger and polydispersed particles;^{32,33} however, this trend was not observed in our systems as the particles appear to be aggregated and polydispersed (see Table 1 and ESI Figure S9).

While the FM:XL ratios of the polymers were not markedly affected by the concentration of initiator in the feed, the T:FM ratio was significantly affected. From 1: 2.5 T:FM ratio obtained from PP-1:1-A, it decreased to 1:6.2 (14% template incorporated) when the I:TM ratio was reduced to 1:200 but increased to 1:3.4 (28% template incorporated) when the I:TM ratio was increased to 1:50. Analyses of the binding capacities of the polymers (Table 1, Figure 6) showed PP-1:1-A (IF = 3.0) to be better performing than both PP-I-1:50 (IF = 2.1) and PP-I-1:200 (IF = 1.2). The drastic reduction in the imprinting and binding efficiencies of PP-I-1:200 compared to PP-1:1-A suggests that slow polymerisation reaction at 60°C does not favour the formation of imprints and merits further investigation. While template incorporation and binding were markedly higher with PP-I-1:50 than with PP-I-1:200, they were still observed to be lower than those for PP-1:1-A. For this reaction, the polymerisation rate was faster as evidenced by the early onset of precipitation, and we speculate that the equilibrium concentration of the TAU-BAAPy complexes has not yet been established. It would seem from our results that, among the I:TM ratios tested, the polymerisation rate resulting from an I:TM ratio of 1:131 used to prepare PP-1:1-A has provided the best precipitation polymerisation condition for imprinting TAU at 60°C.

3.6 | Effect of agitation

Molecular imprinting produced by precipitation polymerisation has been carried out with and without agitation;^{34,35} however, previous studies have illustrated that most systems favour gentle rocking or no form of agitation at all because it assists in the formation of more binding efficient polymers^{33,36} and more mono-dispersed particles.³²

In the case of the precipitation system under study, the effect of agitation, by vigorous stirring (at ~130 rpm) and gentle rolling (at ~9.5 rpm), were investigated under the same conditions as the non-agitated PP-1:1-A. Both polymerisation mixtures subjected to agitation produced highly aggregated particles with a “cauliflower” morphology (ESI Figure S10), consistent with those observed by Yang et al³³ for their particles from stirred precipitation polymerisation mixture. As shown in Tables 1 and S1 (ESI), the conversions and FM:XL ratios (based on EGDMA, measured by qNMR) obtained for these systems varied slightly and, more notably, their T:FM ratios. While PP-1:1-A gave a 1:2.5 stoichiometry, PP-1:1-A-St and PP-1:1-A-Rd afforded 1:1 and 1:2 ratios, respectively. It would seem that agitation has affected the formation of the T:FM association cluster, quite possibly by disrupting the weaker associations but maintaining the strong DAD/ADA hydrogen bond array resulting in a 1:1 (or close to) stoichiometric T:FM ratios. However, while TAU incorporated in PP-1:1-A-St ($173 \pm 3 \mu\text{mol/g}$) is twice higher than that of PP-1:1-A ($98 \pm 3 \mu\text{mol/g}$), PP-1:1-A recorded a binding capacity 10 times higher

($3.64 \pm 0.03 \mu\text{mol/g}$) than the stirred equivalent ($0.29 \pm 0.01 \mu\text{mol/g}$) (Table 1, Figure 6). The higher uptake of the template by PP-1:1-A-St is probably due to “superficial” incorporation of the template which does not necessarily form high fidelity cavities in the polymers. These results suggest that the interaction between the functional monomer and the template is disrupted or reduced when the polymerisation reaction is agitated. On the other hand, the amount of TAU incorporation ($152 \pm 2 \mu\text{mol/g}$) in PP-1:1-A-Rd, which was subjected to a more gentle form of agitation than stirring (rolled at 9.5 rpm), is less than that for PP-1:1-A-St but higher than for PP-1:1-A consistent with the above hypothesis. Conversely, its binding capacity is less than that of PP-1:1-A but higher than that of PP-1:1-A-St.

4 | CONCLUSION

The efficiency of the stoichiometric non-covalent imprinting of BAAPy with TAU due to their strong DAD/ADA hydrogen bond array interaction has been observed in bulk polymerisation process. This study is the first to investigate and assess the imprinting and template rebinding efficiencies of the TAU/BAAPy MIP system prepared by precipitation polymerisation. Template incorporation and batch rebinding as well as polymer composition were measured by quantitative NMR spectroscopy.

We found that the stoichiometric 1:1 T:FM ratio exhibited by the TAU/BAAPy bulk MIP has not been maintained in precipitation polymerisation and a TAU:BAAPy ratio of 1:2.5 was obtained for MIP microspheres prepared in acetonitrile (PP-1:1-A) without agitation from a 1:1 TAU:BAAPy feed. The PP-1:1-A microspheres afforded a K of $1.7 \times 10^4 \text{ M}^{-1}$ and a binding capacity of $3.69 \mu\text{mol/g}$ (41% of the measured incorporated TAU) higher than its bulk counterpart BP-1:1-A ($K = 3.4 \pm 0.3 \times 10^4 \text{ M}^{-1}$, $B_{\text{MIP}} = 4.54 \pm 0.22 \mu\text{mol/g}$) despite incorporating 1.5 times more TAU. Molecular modelling and NMR studies indicate that, aside from the DAD/ADA hydrogen bond interaction, BAAPy also interacts with the acetyl groups of the ribose ring of TAU supporting the formation of the 1:2.5 TAU:BAAPy complex. Non-competitive cross-rebinding and competitive assays using PP-1:1-A against analogue 2,3,5-tri-*O*-acetyl cytidine (TAC), which possess three acetyl groups in the ribose ring but not the imide group, showed significant TAC binding which suggests that BAAPy also interact with the acetyl groups. Nevertheless, cross- and competitive binding assays against uridine resulted in uridine binding higher than that against TAC which indicates that the DAD/ADA hydrogen bond array is the predominant interaction between TAU and BAAPy.

Imprinting efficiency and binding capacity of precipitation MIPs have also been shown to be affected by the initiator concentration and the method of initiation. We found that, for the MIP system under study (PP-1:1-A), the best precipitation polymerisation condition for imprinting TAU at 60°C was provided by a moderate initiator concentration, ie, I:TM ratio of 1:131, also employed by other groups.^{1,4-6,12} Lowering the initiator concentration to achieve an I:TM ratio of 1:200 lowered template incorporation by a factor of 2.6 and binding capacity by a factor of 6.5. On the other hand, increasing the I:TM ratio to 1:50 also reduced template incorporation by 1.3 and binding capacity to 3.2. It is also interesting to note that while vigorous agitation by

stirring showed high template incorporation, it gave very low template rebinding which we found could be improved by mild agitation (gentle rolling at ~9 rpm). However, highest translation of template incorporation to rebinding was obtained with the MIP prepared without agitation which we speculate to be due to the undisrupted and optimal formation of T:FM complexes producing more high fidelity imprints within the polymers. Interestingly, while the imprinting efficiencies (ie, template incorporation with respect to the initial concentration in the polymerisation feed) measured for the better performing TAU MIPs generated in this study were moderate, 41% for PP-1:1-A and 60% for BP-1:1-C, their rebinding capacities were only between 3 and 4% of the incorporated template.

This study also highlights the utility of qNMR for monitoring polymerisation and imprinting efficiencies. Here, we demonstrate the effectivity of the qNMR method for measuring template binding without the need to separate the polymeric particles from the supernatant solution.

ACKNOWLEDGEMENTS

KFL is grateful for the University of Newcastle International (UNIPRS) and Central (UNRSC) Postgraduate Research Scholarships and the technical assistance of Kit-yi Tang (DLS), Dave Phelan (SEM) and Monica Rossignoli (NMR).

ORCID

Clovia I. Holdsworth  <http://orcid.org/0000-0002-6039-0974>

REFERENCES

- Hall AJ, Manesiotis P, Mossing JT, Sellergren B. Molecularly imprinted polymers (MIPs) against uracils: functional monomer design, monomer-template interactions in solution and MIP performance in chromatography. In: *MRS Proceedings*. Cambridge Univ Press: M1; 2002:3.
- Manesiotis P, Hall AJ, Courtois J, Irgum K, Sellergren B. An artificial riboflavin receptor prepared by a template analogue imprinting strategy. *Angew Chem Int Ed*. 2005;44(25):3902-3906.
- Mattos dos Santos P, Hall AJ, Manesiotis P. Stoichiometric molecularly imprinted polymers for the recognition of anti-cancer pro-drug tegafur. *J Chromatogr B*. 2016;1021:197-203.
- Kugimiya A, Mukawa T, Takeuchi T. Synthesis of 5-fluorouracil-imprinted polymers with multiple hydrogen bonding interactions. *Analyst*. 2001;126(6):772-774.
- Krstulja A, Lettieri S, Hall A, Delépée R, Favetta P, Agrofoglio L. Evaluation of molecularly imprinted polymers using 2',3',5'-tri-O-acyluridines as templates for pyrimidine nucleoside recognition. *Anal Bioanal Chem*. 2014;406:6275-6284.
- Manesiotis P, Hall AJ, Sellergren B. Improved imide receptors by imprinting using pyrimidine-based fluorescent reporter monomers. *J Org Chem*. 2005;70(7):2729-2738.
- Yano K, Tanabe K, Takeuchi T, Matsui J, Ikebukuro K, Karube I. Molecularly imprinted polymers which mimic multiple hydrogen bonds between nucleotide bases. *Anal Chim Acta*. 1998;363(2-3):111-117.
- Steinke JHG, Dunkin IR, Sherrington DC. A simple polymerisable carboxylic acid receptor: 2-acrylamido pyridine. *TRAC Trends Anal Chem*. 1999;18(3):159-164.
- Sherrington DC, Taskinen KA. Self-assembly in synthetic macromolecular systems multiple hydrogen bonding interactions. *Chem Soc Rev*. 2001;30(2):83-93.
- Kubo H, Nariai H, Takeuchi T. Multiple hydrogen bonding-based fluorescent imprinted polymers for cyclobarbitol prepared with 2,6-bis(acrylamido)pyridine. *Chem Commun*. 2003;22:2792-2793.
- Tanabe K, Takeuchi T, Matsui J, Ikebukuro K, Yano K, Karube I. Recognition of barbiturates in molecularly imprinted copolymers using multiple hydrogen bonding. *J Chem Soc Chem Commun*. 1995;(22):2303-2304.
- Hall AJ, Manesiotis P, Emgenbroich M, Quaglia M, De Lorenzi E, Sellergren B. Urea host monomers for stoichiometric molecular imprinting of oxyanions. *J Org Chem*. 2005;70(5):1732-1736.
- Beltran A, Borrull F, Cormack PAG, Marcé RM. Molecularly imprinted polymer with high-fidelity binding sites for the selective extraction of barbiturates from human urine. *J Chromatogr A*. 2011;1218(29):4612-4618.
- Esfandiyari-Manesh M, Javanbakht M, Atyabi F, Badii A, Dinarvand R. Effect of porogenic solvent on the morphology, recognition and release properties of carbamazepine-molecularly imprinted polymer nanospheres. *J Appl Polym Sci*. 2011;121(2):1118-1126.
- Tm P, Horváth V, Tolokán A, Horvai G, Sellergren B. Effect of solvents on the selectivity of terbutylazine imprinted polymer sorbents used in solid-phase extraction. *J Chromatogr A*. 2002;973(1-2):1-12.
- Renkecz T, László K, Horváth V. Molecularly imprinted microspheres prepared by precipitation polymerization at high monomer concentrations. In: *Molecular Imprinting*. 2014;2:1-17.
- Beijer FH, Sijbesma RP, Vekemans JAJM, Meijer EW, Kooijman H, Spek AL. Hydrogen-bonded complexes of diaminopyridines and diaminotriazines: opposite effect of acylation on complex stabilities. *J Org Chem*. 1996;61(18):6371-6380.
- Minch MJ. An introduction to hydrogen bonding (Jeffrey, George A.). *J Chem Educ*. 1999;76(6):759.
- Carro-Díaz AM, Lorenzo-Ferreira RA. Molecularly imprinted polymers for sample preparation. In: *Handbook of Molecularly Imprinted Polymers*. Shrewsbury, U.K: Smithers Rapra Publishing; 2013.
- Pan G, Zu B, Guo X, Zhang Y, Li C, Zhang H. Preparation of molecularly imprinted polymer microspheres via reversible addition-fragmentation chain transfer precipitation polymerization. *Polymer*. 2009;50(13):2819-2825.
- Ansell R. Characterization of the binding properties of molecularly imprinted polymers. In: *Molecularly Imprinted Polymers in Biotechnology*. Switzerland: Springer International Publishing; 2015:51-93.
- Ye L, Weiss R, Mosbach K. Synthesis and characterization of molecularly imprinted microspheres. *Macromolecules*. 2000;33(22):8239-8245.
- Cacho C, Turiel E, Martín-Esteban A, Pérez-Conde C, Cámara C. Characterisation and quality assessment of binding sites on a propazine-imprinted polymer prepared by precipitation polymerisation. *J Chromatogr B*. 2004;802(2):347-353.
- Chen L, Xuab S, Li J. Recent advances in molecular imprinting technology: a current status, challenges and highlighted applications. *Chem Soc Rev*. 2011;40:2922-2942.
- Wang J-Y, Liu F, Xu Z-L, Li K. Theophylline molecular imprint composite membranes prepared from poly(vinylidene fluoride) (PVDF) substrate. *Chem Eng Sci* 2010; 65(10):3322-3330.
- Ju H, Xueji Z, Wang J. *NanoBiosensing: Principles, Development and Application*. New York: Springer; 2011.
- Mohajeri SA, Karimi G, Aghamohammadian J, Khansari MR. Clozapine recognition via molecularly imprinted polymers; bulk polymerization versus precipitation method. *J Appl Polym Sci*. 2011;121(6):3590-3595.
- Umpleby Ii RJ, Baxter SC, Rampey AM, Rushton GT, Chen Y, Shimizu KD. Characterization of the heterogeneous binding site affinity distributions in molecularly imprinted polymers. *J Chromatogr B*. 2004; 804(1):141-149.
- Turiel E, Perez-Conde C, Martín-Esteban A. Assessment of the cross-reactivity and binding sites characterisation of a propazine-imprinted

- polymer using the Langmuir-Freundlich isotherm. *Analyst*. 2003; 128(2):137-141.
30. Mijangos I, Navarro-Villoslada F, Guerreiro A, et al. Influence of initiator and different polymerisation conditions on performance of molecularly imprinted polymers. *Biosens Bioelectron*. 2006;22(3):381-387.
31. Piletsky SA, Mijangos I, Guerreiro A, et al. Polymer cookery: influence of polymerization time and different initiation conditions on performance of molecularly imprinted polymers. *Macromolecules*. 2005; 38(4):1410-1414.
32. Wang J, Cormack PA, Sherrington DC, Khoshdel E. Synthesis and characterization of micrometer-sized molecularly imprinted spherical polymer particulates prepared via precipitation polymerization. *Pure Appl Chem*. 2007;79(9):1505-1519.
33. Yang S, Shim SE, Lee H, Kim GP, Choe S. Size and uniformity variation of poly(MMA-co-DVB) particles upon precipitation polymerization. *Macromolecular Research*. 2004;12(5):519-527.
34. Ye L, Mosbach K, Krozerc A, Reinmultc K, Yoshimatsu K. Uniform molecularly imprinted microspheres and nanoparticles prepared by precipitation polymerization: the control of particle size suitable for different analytical applications. *Anal Chim Acta*. 2007;584:112-121.
35. Ye L, Mosbach K. Molecularly imprinted microspheres as antibody binding mimics. *React Funct Polym*. 2001;48(1-3):149-157.
36. Kotrotsiou O, Chaitidou S, Kiparissides C. Boc-l-tryptophan imprinted polymeric microparticles for bioanalytical applications. *Mater Sci Eng C*. 2009;29(7):2141-2146.

SUPPORTING INFORMATION

Additional Supporting Information may be found online in the supporting information tab for this article.

How to cite this article: Lim KF, Hall AJ, Lettieri S, Holdsworth CI. Assessment of the imprinting efficiency of an imide with a "stoichiometric" pyridine-based functional monomer in precipitation polymerisation. *J Mol Recognit*. 2018;31:e2655. <https://doi.org/10.1002/jmr.2655>